All-Fiber Passively Q-Switched Laser Based on Tm^{3+}-Doped Tellurite Fiber

Pei-Wen Kuan, Kefeng Li, Lei Zhang, Xiaokang Fan, Tawfique Hasan, Fengqiu Wang, and Lili Hu

***Abstract*— We report all-fiber passively Q-switched Tm^{3+}-doped tellurite fiber lasers. The composite tellurite fiber is specially designed to improve the mechanical strength. Both carbon nanotubes (CNTs) and semiconductor saturable absorber mirror (SESAM) are inserted separately into the laser cavities as SAs to demonstrate a fiber-integrated setup. In a short, 9-cm tellurite fiber, 1.86-μm-pulsed lasers without self-mode-locking effect are demonstrated by in-band pumping at 1.59 μm. An average power of 84 mW is obtained in CNT-pulsed laser with 860-ns duration, whereas in SESAM-pulsed laser, the average power reaches 21 mW with 516-ns pulsewidth.**

***Index Terms*— Tellurite glass fiber, fiber lasers, Q-switching.**

I. Introduction

PULSED Tm^{3+}-doped fiber lasers operating in eye-safe $\sim$2 μm wavelength region have recently attracted significant attention owing to their wide range of potential applications [1]–[4]. Among various means for pulse modulation, passive Q-switching is a favorable approach to pulsed lasers due to its advantages in terms of cost, simplicity, efficient operation and high pulse energy. Passive Q-switched Tm-doped fiber lasers typically possess microsecond- or nanosecond-order pulses. Such long pulse durations are ideal for coherent laser LiDAR, and also serve to reduce the risks of damage to optical elements due to high intracavity fluencies [5], [6]. Thanks to recent developments of saturable absorber (SA) materials, passively Q-switched pulse lasers have been realized by utilizing CNTs [7], graphene [8], SESAMs [9], Cr^{2+}:ZnSe crystals [10], metal dichalcogenides [11], rare-earth doped fibers [12], *etc*.

Manuscript received November 8, 2014; revised December 10, 2014; accepted December 18, 2014. Date of publication December 24, 2014; date of current version March 2, 2015. This work was supported in part by the Natural Science Foundation of Shanghai under Grant 12ZR1451600, in part by the National Natural Science Foundation of China under Grant 61308084, and in part by the Granted Membership of Youth Innovation Promotion Association through the Chinese Academy of Sciences, Beijing, China. *(Corresponding author: Kefeng Li.)*

P.-W. Kuan and X. Fan are with the Key Laboratory of Materials for High Power Laser, Shanghai Institute of Optics and Fine Mechanics, Chinese Academy of Sciences, Shanghai 200050, China, and also with the University of Chinese Academy of Sciences, Beijing 100049, China (e-mail: peiwenkuan@gmail.com; fxk198811@163.com).

K. Li, L. Zhang, and L. Hu are with the Key Laboratory of Materials for High Power Laser, Shanghai Institute of Optics and Fine Mechanics, Chinese Academy of Sciences, Shanghai 200050, China (e-mail: kfli@siom.ac.cn; leizhju@siom.ac.cn; hulili@siom.ac.cn).

T. Hasan is with the Cambridge Graphene Centre, University of Cambridge, Cambridge CB2 1TN, U.K. (e-mail: th270@cam.ac.uk).

F. Wang is with the Department of Electronic Science and Engineering, Nanjing University, Nanjing 210023, China (e-mail: fwang@nju.edu.cn).

Color versions of one or more of the figures in this letter are available online at http://ieeexplore.ieee.org.

Digital Object Identifier 10.1109/LPT.2014.2385812

By virtue of the mature fabrication process, Tm^{3+}-doped silica glass based fibers have dominated this research. However, multi-component glasses providing intrinsic advantages have been intensively investigated as fiber host glass materials, and further applied to pulsed laser generation. For example, Tm-doped fluoride and Tm/Ho co-doped tellurite fiber lasers have been Q-switched by acousto-optic modulator [13] and mechanical chopper [14], respectively. In highly Tm-doped silicate fiber and germinate fiber, $\sim$2 μm single-frequency Q-switched lasers were demonstrated by using stress-induced birefringence [15], [16]. A high repetition rate mode-locking operation was also achieved in the silicate fiber [17]. Nevertheless, hardly any passive Q-switched lasers using multi-component glass fibers have been demonstrated.

High refractive index, high rare earth solubility, low phonon energy, and wide transmission region makes tellurite glasses promising hosts for laser fibers and mid-infrared transport fibers [18]. However, the brittleness of tellurite fibers is a critical limitation for their practical applications. In our previous study, a composite glass fiber structure was demonstrated successfully to improve the mechanical strength of tellurite fibers [19]. Joining of fibers with different materials is also challenging. Different techniques can be employed to address this. For example, Ohishi *et al*. employed the thermally diffused expanded core (TEC) and tilted V-groove connection techniques to achieve low-loss and low-reflection splicing between the tellurite-based erbium-doped fiber and high numerical aperture (NA) silica fiber [20]. In practice, though commercial fusion splicers are available, the process of splicing two different fibers is complex. Due to this, $\sim$2 μm tellurite fiber lasers have only been employed through complicated free-space coupling scheme till now.

In this letter, a composite tellurite fiber has been designed to match the commercial silica fiber (Corning, SMF-28). A purpose-built homemade tellurite fiber jumper is applied to connect the tellurite and silica fiber in a flange, forming a stable and simple all-fiber laser configuration. Using CNT films and SESAM, $\sim$2 μm passively Q-switched tellurite fiber laser is investigated for the first time. With in-band pumping configuration, a maximum average power of $\sim$84 mW with 0.86 μs time duration and 736 nJ energy is achieved from a 9 cm long tellurite fiber, without any instability from Q-switched mode-locking.

II. Experimental Setup and Result

The composite single-mode tellurite fiber used in this letter is made in house by rod-in-tube method. Owing to the

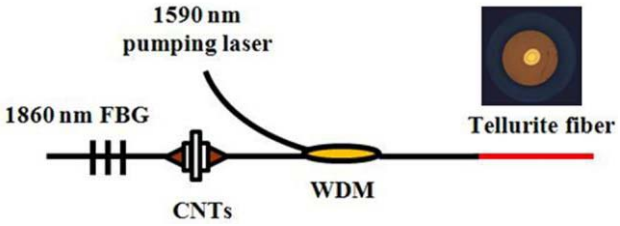

Fig. 1. Schematic of Q-switched Tm^{3+}-doped tellurite fiber laser inserted with fiber cross-section.

similar softening temperature (~500 °C) and thermal expansion (~100×10^{-7}/°C) of tellurite and phosphate glasses, the latter glass is utilized as the outer cladding to promote the robustness and practicality of the tellurite fiber. The fiber has a core diameter of 8.3 μm with 0.14 NA, and a 125 μm cladding diameter, matching the SMF-28 fiber well. The core is uniformly doped with 1 mol. % Tm_2O_3 (Tm^{3+}: 3.76×10^{20} ions/cm^3). The propagation loss is ~2 dB/m at 1310 nm, and the mode field diameter is ~7.2 μm at 1860 nm. A tellurite fiber module with an optimized length of 9 cm is prepared as the gain medium in our Q-switched laser cavities. Both ends of the tellurite fiber are inserted into ceramic ferrules which are perpendicularly cleaved and well-polished. Employing physical contact in this module enables easy and optimum in-line fiber connection. The total attenuation of tellurite fiber module is estimated as ~6 dB at 1590 nm using the insertion-loss method. The pump source is an Er/Yb co-doped single-mode fiber (Nufern) laser operating at 1590 nm. This is close to the absorption peak of the Tm^{3+}: $^3H_6 \rightarrow {}^3F_4$ transition, which provides a low quantum defect heating and prevents pump excited-state absorption. With CNTs and SESAM as SAs, the behavior of pulsed laser is presented and discussed in the following part.

A. CNTs Based Q-Switched Tellurite Fiber Laser

The experimental setup for our CNT-based passively Q-switched tellurite fiber laser is shown in Fig. 1. The linear laser oscillator is comprised of Tm^{3+}-doped composite tellurite fiber, a fiber Bragg grating (FBG) with high-reflection (>99%) at 1860 nm, a wavelength division multiplexer (WDM), and a piece of CNT-polyvinyl alcohol (PVA) film. The sample used here is double wall CNTs, with 1.1 and 1.8nm inner and outer diameters, respectively [21]. The composite has been prepared from the CNT aqueous dispersions according to the procedure described in Ref [21]. The total length of the fiber laser cavity is ~2.8 m. The tellurite fiber output end which has a ~11.9% Fresnel reflection, is used as an output coupler. To prevent the remaining pump light from damaging SAs, the CNT-PVA film is placed on to the pass port of WDM and sandwiched between two fiber connectors, to form a fiber-compatible SA integrated into the laser cavity. Fig. 2 shows the absorption spectrum (red) of the CNT-PVA. The ~2μm absorption band has a peak width of ~350 nm. The output 1860 nm laser is measured using a StellarNet RED-Wave NIRx spectrometer. The pulse signal is monitored by an InGaAs photodetector (DET10D, Thorlabs) and a 2 GHz sampling rate oscilloscope (MSO4104, Tektronix).

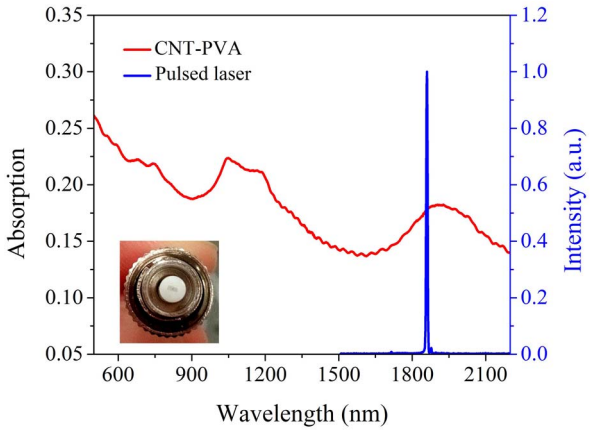

Fig. 2. Absorption spectrum of CNT-PVA film and 1860 nm laser output of Q-switched laser.

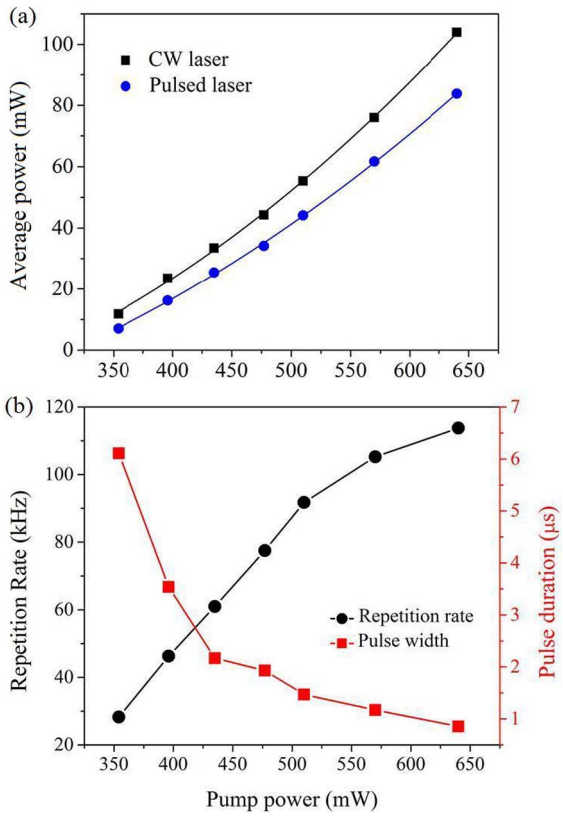

Fig. 3. (a) Average output power of CW and pulsed lasers as function of incident pump power at 1860 nm. (b) Pulse repetition rate and pulse width versus the incident pump power.

Figure 3(a) shows the average output powers at 1860 nm with respect to the incident pump power in continuous wave (CW) and Q-switched operations. The CW performance at 1860 nm provides the baseline for efficiency evaluation of the passively Q-switched setup. Without the CNT SA in the cavity, the CW 1860 nm laser output is 104 mW at an incident pump power of 640 mW in the fiber module. The slope efficiency is ~31.5%, comparable to the result reported by ref. [18] with a similar laser scheme (*i.e.* a 10 cm fiber in-band pumped at 1.6 μm in a 99%–12% cavity).

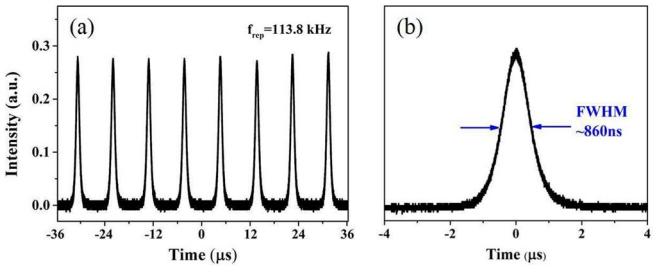

Fig. 4. (a) Typical pulse train and (b) single pulse shape at incident pump power of 640 mW from our CNT Q-switched laser.

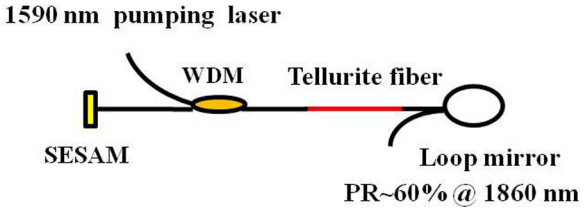

Fig. 5. Setup of SESAM Q-switched tellurite fiber laser. (PR: Partial reflectivity).

For CNT Q-switching, an average output power of 84 mW is obtained at an incident pump power of 640 mW, corresponding to a slope efficiency of 26.3%. As a consequence, the Q-switching efficiency (ratio of the Q-switched output power to the CW power at the maximum pump power) is estimated to be as high as 80.7%. This Q-switching extraction efficiency is superior to those of the lasers with Cr^{2+}-doped crystals (~17–61.3% efficiency) used as SAs [10], [22].

Figure 3(b) reveals the pulse repetition rate and the pulse duration versus the incident pump power at 1860 nm. With increasing pump power, the repetition rate increases monotonically from 28.3 to 113.8 kHz. As for the pulse width, it reduces from 6.11 to 0.86 μs. The oscilloscope trace of the CNT Q-switched pulse train and single pulse envelope at a pump power of 640 mW is shown in Fig. 4. The corresponding single pulse energy is 736 nJ.

B. SESAM Based Q-Switched Fiber Laser

For SESAM Q-switching, the experimental setup is presented in Fig. 5. The tellurite module with 9 cm fiber length is used. A laser resonator is formed by a commercial SESAM and a fiber loop mirror. The fiber end facet of WDM pass port is butted directly to the SESAM (SAM-1920-36-10ps, BATOP). The low intensity reflectance at 1860 nm of SESAM is ~61%. The fiber loop mirror, fabricated with a 1550 nm 3dB coupler, has an estimated reflectivity of ~60%. The output fiber of loop mirror has an 8° angled end to suppress the feedback light. The total cavity length is ~2.2 m.

Figure 6(a) shows the average output power at 1860 nm and estimated pulsed energy with respect to the incident pump power. The maximum average output power is 21.4 mW. The ~4.6% slope efficiency is much lower than that of the CNT Q-switched laser. It can be attributed to the lower output coupling, higher initial absorbance, and higher insertion losses in the laser cavity. The insertion losses are mainly from the connection between tellurite fiber and silica fiber, caused

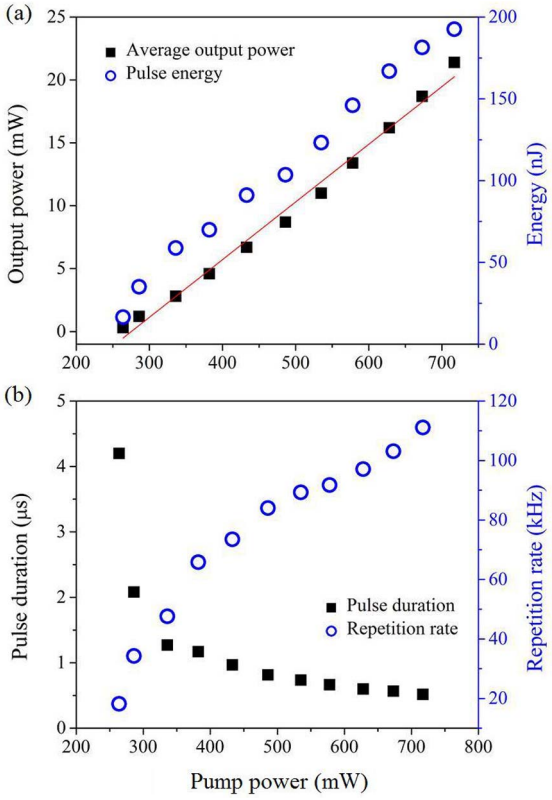

Fig. 6. (a) Average output power, pulse energy, (b) pulse duration, and repetition rate of SESAM Q-switched laser versus the incident pump power.

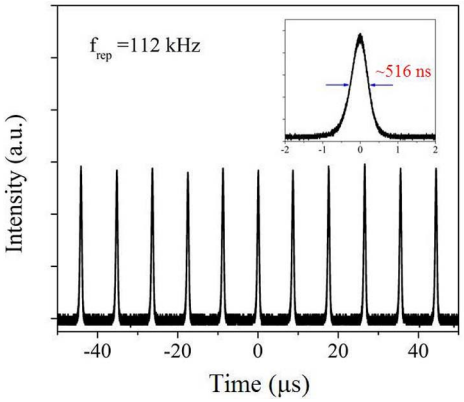

Fig. 7. Temporal shape of Q-switched pulse train and single pulse envelope with incident pump power of 717 mW.

from the mismatch of mode field diameter, refractive index, and concentric alignment [23]. The dependence of the pulse width and the pulse repetition rate on the incident pump power is shown in Fig. 6(b). The pulse duration decreases from 4.2 μs to 516 ns, and repetition rate increases from 18.2 to 111.2 kHz when the incident pump power increases from 264 to 717 mW. A pulse train of SESAM Q-switched laser at a maximum pump power of 717 mW is shown in Fig. 7. The inset presents the shortest pulse duration of 516 ns, corresponding to a single pulse energy of 192.6 nJ. The interpulse intensity fluctuation is less than 10%.

A suitable condition for Q-switching operation can be expressed as [24]: $I \times |dR/dI| > T_R/\tau$, where R is the absorber

reflectivity, I is the laser intensity on the absorber, *dR/dI* is the saturation intensity, τ is the stimulated life time of upper laser level, and T_R is the cavity round trip time. The authors point out that short cavity length for small T_R and long upper state lifetime are easier for Q-switching. The upper state lifetime of Tm^{3+}-doped tellurite fiber in the range of several milliseconds is preferable to that of silica fibers in hundreds of microseconds [25]. Moreover, the additional stability requirement has to be fulfilled to prevent Q-switched mode-locking. In our CNT Q-switched laser, the narrowband fiber grating is used to suppress the self-mode-locking effect [26]. Although the fiber loop mirror provides a wideband gain-reflection in SESAM Q-switched laser, the phenomenon of Q-switched mode-locking is still absent. The instability from Q-switched mode-locking can be prevented if $E_p^2 > E_{sat,L} E_{sat,A} \Delta R$ [27] where E_p is intercavity energy, $E_{sat,L}$ is saturation energy of laser ($\propto A_{eff}/\sigma_{em,L}$), $E_{sat,A}$ is saturation energy of the absorber, and ΔR is modulation of SA. Therefore, A_{eff}, the average mode area inside the laser medium should be small and $\sigma_{em,L}$, the emission cross-section of gain material should be large. In accordance with the Fuchtbauer–Ladenburg formula, the emission cross-section is related to refractive index that can be described as $\sigma_{em} \propto (n^2+2)^2/9$ [28], [29]. Accordingly, the tellurite fiber with high refractive index ($\sim$2.0) [25] and small mode-field area could lead to small value of $E_{sat,L}$ to meet the above criteria. By enhancing the doping concentration and the fiber concentricity, the pump absorption could be further ameliorated, making a shorter active fiber adequate. Also, the SAs can be placed in common port of WDM due to lower remaining pump power. Thus, shorter laser cavity could be formed to shorten the pulse duration and obtain better Q-switching performance.

III. Conclusion

In conclusion, we demonstrate the first passively Q-switched Tm^{3+}-doped tellurite fiber laser. In all-fiber configuration, 84 mW average power is obtained with CNT-based Q-switched laser in a 9 cm fiber. The pulse energy is 736 nJ with 860 ns width. On the other hand, the output power of SESAM-based Q-switched laser reaches 21 mW with 516 ns width, with 193 nJ corresponding pulse energy. The pulse duration and repetition rate can be tuned by changing the pump power. Higher efficiency and shorter pulse may be achieved by further optimization of the fiber configuration and enhancement of the pump absorption.

References

[1] J. Geng, Q. Wang, and S. Jiang, "2 μm fiber laser sources and their applications," *Proc. SPIE*, vol. 8164, pp. 816409-1–816409-10, Sep. 2011.

[2] J. Yang, Y. Tang, and J. Xu, "Development and applications of gain-switched fiber lasers [Invited]," *Photon. Res.*, vol. 1, no. 1, pp. 52–57, 2013.

[3] X. Wang, P. Zhou, X. Wang, H. Xiao, and L. Si, "51.5 W monolithic single frequency 1.97 μm Tm-doped fiber amplifier," *High Power Laser Sci. Eng.*, vol. 1, nos. 3–4, pp. 123–125, 2013.

[4] X. Wang, P. Zhou, X. Wang, H. Xiao, and Z. Liu, "Bursts with shape-alterable pulses in a compact Tm-doped fiber laser with simultaneous active intracavity phase and intensity modulations," *Photon. Res.*, vol. 2, no. 6, pp. 172–176, 2014.

[5] S. W. Henderson *et al.*, "Coherent laser radar at 2 μm using solid-state lasers," *IEEE Trans. Geosci. Remote Sens.*, vol. 31, no. 1, pp. 4–15, Jan. 1993.

[6] M. G. Jani, N. P. Barnes, K. E. Murray, F. L. Naranjo, and G. E. Lockard, "Diode-pumped long-pulse-length Ho:Tm:$YLiF_4$ laser at 10 Hz," *Opt. Lett.*, vol. 20, no. 8, pp. 872–874, 1995.

[7] T. Hasan *et al.*, "Nanotube–polymer composites for ultrafast photonics," *Adv. Mater.*, vol. 21, nos. 38–39, pp. 3874–3899, 2009.

[8] D. Popa, Z. Sun, T. Hasan, F. Torrisi, F. Wang, and A. C. Ferrari, "Graphene Q-switched, tunable fiber laser," *Appl. Phys. Lett.*, vol. 98, no. 7, p. 073106, 2011.

[9] X. Yin, J. Meng, J. Zu, and W. Chen, "Semiconductor saturable-absorber mirror passively Q-switched Yb:YAG microchip laser," *Chin. Opt. Lett.*, vol. 11, no. 8, p. 081402, 2013.

[10] Y. Tang, Y. Yang, J. Xu, and Y. Hang, "Passive Q-switching of short-length Tm^{3+}-doped silica fiber lasers by polycrystalline Cr^{2+}:ZnSe microchips," *Opt. Commun.*, vol. 281, no. 22, pp. 5588–5591, 2008.

[11] R. I. Woodward *et al.*, "Q-switched fiber laser with MoS_2 saturable absorber," in *Proc. CLEO*, San Jose, CA, USA, 2014, pp. 1–3, paper SM3H.6.

[12] S. D. Jackson, "Passively Q-switched Tm^{3+}-doped silica fiber lasers," *Appl. Opt.*, vol. 46, no. 16, pp. 3311–3317, 2007.

[13] M. Eichhorn, "Development of a high-pulse-energy Q-switched Tm-doped double-clad fluoride fiber laser and its application to the pumping of mid-IR lasers," *Opt. Lett.*, vol. 32, no. 9, pp. 1056–1058, 2007.

[14] Y. Tsang, B. Richards, D. Binks, J. Lousteau, and A. Jha, "Tm^{3+}/Ho^{3+} codoped tellurite fiber laser," *Opt. Lett.*, vol. 33, no. 11, pp. 1282–1284, 2008.

[15] J. Geng, Q. Wang, J. Smith, T. Luo, F. Amzajerdian, and S. Jiang, "All-fiber Q-switched single-frequency Tm-doped laser near 2 μm," *Opt. Lett.*, vol. 34, no. 23, pp. 3713–3715, 2009.

[16] W. Shi *et al.*, "220 μJ monolithic single-frequency Q-switched fiber laser at 2 μm by using highly Tm-doped germanate fibers," *Opt. Lett.*, vol. 36, no. 18, pp. 3575–3577, 2011.

[17] Q. Wang, J. Geng, T. Luo, and S. Jiang, "2 μm mode-locked fiber lasers," *Proc. SPIE*, vol. 8237, pp. 82371N-1–82371N-8, Feb. 2012.

[18] B. Richards, Y. Tsang, D. Binks, J. Lousteau, and A. Jha, "Efficient $\sim$ 2 μm Tm^{3+}-doped tellurite fiber laser," *Opt. Lett.*, vol. 33, no. 4, pp. 402–404, 2008.

[19] K. Li *et al.*, "In-band pumping of Tm doped single mode tellurite composite fiber," *Proc. SPIE*, vol. 8982, pp. 89821M-1–89821M-6, Mar. 2014.

[20] M. Yamada *et al.*, "Gain-flattened tellurite-based EDFA with a flat amplification bandwidth of 76 nm," *IEEE Photon. Technol. Lett.*, vol. 10, no. 9, pp. 1244–1246, Sep. 1998.

[21] T. Hasan *et al.*, "Double-wall carbon nanotubes for wide-band, ultrafast pulse generation," *ACS Nano*, vol. 8, no. 5, pp. 4836–4847, 2014.

[22] J. Y. Huang, H. C. Liang, K. W. Su, and Y. F. Chen, "High power passively Q-switched ytterbium fiber laser with Cr^{4+}:YAG as a saturable absorber," *Opt. Exp.*, vol. 15, no. 2, pp. 473–479, 2007.

[23] M. Kihara. (Jun. 13, 2013). *Current Developments in Optical Fiber Technology*. [Online] Available: http://www.intechopen.com/

[24] G. J. Spühler *et al.*, "Experimentally confirmed design guidelines for passively Q-switched microchip lasers using semiconductor saturable absorbers," *J. Opt. Soc. Amer. B*, vol. 16, no. 3, pp. 376–388, 1999.

[25] K. Li, G. Zhang, and L. Hu, "Watt-level $\sim$ 2 μm laser output in Tm^{3+}-doped tungsten tellurite glass double-cladding fiber," *Opt. Lett.*, vol. 35, no. 24, pp. 4136–4138, 2010.

[26] C. Liu *et al.*, "High-energy passively Q-switched 2 μm Tm^{3+}-doped double-clad fiber laser using graphene-oxide-deposited fiber taper," *Opt. Exp.*, vol. 21, no. 1, pp. 204–209, 2013.

[27] U. Keller, "Recent developments in compact ultrafast lasers," *Nature*, vol. 424, pp. 831–838, Aug. 2003.

[28] X. Li, X. Liu, L. Zhang, L. Hu, and J. Zhang, "Emission enhancement in Er^{3+}/Pr^{3+}-codoped germanate glasses and their use as a 2.7-μm laser material," *Chin. Opt. Lett.*, vol. 11, no. 12, pp. 121601-1–121601-3, 2013.

[29] X. Liu *et al.*, "$\sim$ 2 μm luminescence properties and nonradiative processes of Tm^{3+} in silicate glass," *J. Lumin.*, vol. 150, pp. 40–45, Jun. 2014.